Computer Physics Communications 182 (2011) 2479–2485

Contents lists available at ScienceDirect

Computer Physics Communications

www.elsevier.com/locate/cpc

Efficient numerical method for linear stability analysis of solitary waves

Adrian Alexandrescu [a,*], José R. Salgueiro [b]

[a] Avda. del Mediterraneo 16, 7D Derecha, Madrid 28007, Spain
[b] Área de Óptica, Departamento de Física Aplicada, Universidade de Vigo, As Lagoas s/n, Ourense 32004, Spain

ARTICLE INFO

Article history:
Received 26 January 2011
Received in revised form 1 June 2011
Accepted 6 July 2011
Available online 21 July 2011

Keywords:
Nonlinear waves
Linear stability
Complex eigenvalues
Relaxation algorithm

ABSTRACT

In this paper we use a numerical relaxation algorithm to improve and generalize the obtainment of the perturbation eigenstates of nonlinear systems. As a model problem we consider the linear stability analysis of the vortex eigenstates of the cubic–quintic nonlinear Schrödinger equation. It is shown by numerical calculations that the relaxation algorithm permits accurate tracing of complex perturbation eigenvalues.

1. Introduction

Nonlinear equations arise in general from many-particle interactions where the reformulation of the initial problem is required in order to obtain a tractable model. Nonlinear wave equations were formulated for a wide range of phenomena, including crystal dislocation, matter–light interaction, Bose–Einstein condensation and dynamics of biological molecules [1]. The study of nonlinear wave equations addresses many issues ranging from purely theoretical aspects, e.g. existence, uniqueness of their solutions, their construction or stability to their experimental probing. Stable nonlinear waves maintain their features, for example localization or shape, almost unchanged while the unstable ones may display collapse, delocalization or splitting. Stability criteria like energetic, dynamical and linear stability [2] may help in the characterization of the dynamics of the waves. The energetic and dynamical stability are responsible for the behavior upon finite non-small perturbations and is mainly studied using analytical methods, being tractable only in some particular situations (see for instance Refs. [2,3] and references therein). The linear stability analysis is used to investigate the behavior upon infinitesimally small perturbations. The energetic criteria is the strongest one and is based on global properties of the Hamiltonian structure of the system, while the linear criteria is the weakest one. In general the stability analysis of nonlinear waves is a challenging task and may involve a combination of analytical and/or numerical methods whose results are to be cross-checked in order to validate them. The stability analysis for different kinds of nonlinear waves was extensively treated in the literature, including those in media showing Kerr [2], saturable [4,5], cubic–quintic [6] or even more complicated nonlinearities [7].

The issue of linear stability reduces to the analysis of an eigenvalue problem obtained by linearizing the original nonlinear problem. Analytical methods for linear stability analysis are based mainly on the spectral properties of operators [2,3,5]. The number of numerical algorithms for linear eigenvalue problems makes somewhat easier this approach as they can be used to determine any kind of eigenvalue, i.e. real, imaginary or complex. Nevertheless, one has to dedicate some extra effort in distinguishing physical eigenvalues from the spurious ones. This may turn into a difficult task in the case of purely numerical problems. Another successful approach is to determine the eigenvalues by monitoring the growth of unstable modes as they evolve [4]. Although this method permits a straightforward interpretation of the results by capturing the dominant perturbation, i.e. the one showing fastest growing, it turns out to be inappropriate for determining slow growing, non-dominant or oscillating perturbations.

In this paper we describe an additional method for the study of the stability of nonlinear systems based on a numerical relaxation method for two-point boundary value problems [8]. The method does not suffer from the drawbacks of the eigenvalue or growth rate methods. The only requirement is a good initial guess of the perturbation to be determined, which can be provided by one of the above mentioned methods applied for a non-problematic set of parameters. The convergence obtained from the initial guess makes possible the calculation of many different eigenstates in a row by slightly varying the values of the parameters. This method has been successfully used in the linear stability analysis of solitary

* Corresponding author.
E-mail addresses: adrian.alexandrescu2000@gmail.com (A. Alexandrescu), jrs@uvigo.es (J.R. Salgueiro).

0010-4655/$ – see front matter
doi:10.1016/j.cpc.2011.07.006

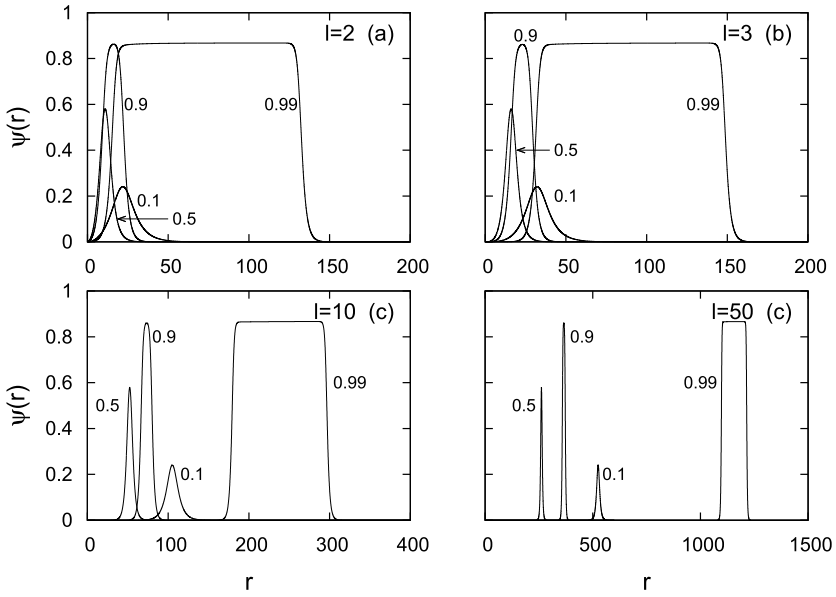

Fig. 1. Stationary vortex states of the nonlinear Schrödinger equation with cubic–quintic nonlinearity having the azimuthal charge $l = 2, 3, 10$ and 50, and the propagation constant $\beta/\beta_{cr} = 0.1, 0.5, 0.9$ and 0.99.

waves propagating in nonlinear coherent media [7]. A similar technique may be applied using other iterative methods [9].

To present the main aspects of the algorithm and illustrate its performance we chose as a model problem the cubic–quintic nonlinear Schrödinger equation (CQNLS) [10,11]. A good reason for this choice was the controversy that this system originated in the past basically because of its numerical complexity. In fact, an uncareful choice of the propagation step and/or the sampling mesh was probably the reason why erroneous results were reported using the growth rate perturbation method [12,13]. Close to the critical point, where the stationary states take the top-flat shape and their instability vanishes, the numerical problem requires from a big computational effort and this situation can be easily managed by the proposed relaxation method.

The organization of this paper is as follows. In Section 2 we briefly present the main aspects of the linear stability analysis for nonlinear systems. In Section 3 we describe the model problem that will be used to illustrate the calculation method. In Section 4 we detail the proposed method and discuss the obtained results. Finally, in Section 5 the main results are summarized and future extensions are discussed.

2. Linear stability analysis

Linear stability analysis is one of the most successful methods of evaluating the stability of nonlinear systems [1,3]. Basically, the linear stability follows the development, e.g. growth, oscillation or suppression, of arbitrary small induced perturbations. In order to carry out the calculation the perturbed field is substituted in the equation describing the physical phenomenon which is further linearized in order to obtain a relationship for the perturbation. In that way it is usually obtained an eigenvalue problem which, once solved, provides the growth rate of the different instabilities affecting the physical system. The growth can be negative in all cases, revealing that the system if fully stable – at least in a linear perturbation context – or there can exist positive growing eigenvalues, being the highest of them the one which dominates the instability scenario. For an overview of the linear stability analysis in optical solitary waves see Ref. [3].

The linear stability analysis can be undertaken in any situation by numerical methods and only in some particular situations by analytical methods, e.g. one-dimensional scenarios or simple nonlinearities. The results of the linear stability analysis are significant because only stable or weakly unstable solitary waves can be probed experimentally.

3. The model problem: Schrödinger equation with cubic–quintic nonlinearity

As a model problem to illustrate and test the proposed method we use the cubic–quintic nonlinear Schrödinger (CQNLS) equation of $(2D + 1)$ form with two transverse dimensions and one evolution dimension:

$$i\frac{\partial \psi}{\partial z} + \Delta_\perp \psi + n_2|\psi|^2\psi - n_4|\psi|^4\psi = 0 \tag{1}$$

where $\Delta_\perp$ is the two-dimensional Laplace operator and n_2 and n_4 the strictly positive coefficients of the nonlinear terms. The stationary states of Eq. (1) with azimuthal charge l and propagation constant β, also known as *vortex states*, can be written as

$$\psi(\mathbf{r}, z) \equiv \psi(r)e^{i(l\varphi+\beta z)} \tag{2}$$

where $\mathbf{r} = (r, \varphi)$, $r = \sqrt{x^2 + y^2}$, $\varphi = \tan^{-1}(y/x)$ and $\beta > 0$. We maintain for convenience the same notation ψ for the radial dependence of the solution. Inserting the above vortex state into the time dependent Eq. (1) one obtains the stationary equation,

$$\Delta_r \psi - \frac{l^2}{r^2}\psi + n_2|\psi|^2\psi - n_4|\psi|^4\psi - \beta\psi = 0 \tag{3}$$

where $\Delta_r = d^2/dr^2 + (1/r)\,d/dr$. Finite norm $N = \int dx\,dy|\psi|^2 < \infty$ solutions of Eq. (3) are found for propagation constant β in the range $(0, \beta_{cr})$ with $\beta_{cr} = 3n_2^2/16n_4$ [13,14]. In the subsequent numerical calculations we set $n_2 = n_4 = 1$ which leads to $\beta_{cr} = 0.1875$. For values of β close to zero the stationary states of Eq. (3) resemble those of the cubic nonlinear Schödinger equation. As we approach the critical value β_{cr} the defocusing quintic nonlinearity leads to the saturation of the maximum amplitude while the norm grows by an increasing spatial radial width [13]. The stationary states described by Eq. (3) can be calculated using for instance the shooting [18], relaxation [13], imaginary time evolution [15], fixed-point [16] or gradient-conjugate methods [17]. Fig. 1 gives an overview of the various stationary vortex states for several values

of the azimuthal charge l and the eigenvalue β. The properties of Eqs. (1) and (3) were extensively studied theoretically and numerically – see for instance Ref. [19] for a somewhat comprehensive list of the published works.

3.1. Linear stability analysis for the model problem

The linear stability is addressed by considering a slightly perturbed stationary state $\tilde{\psi}(r)$ of the following form [20]:

$$\tilde{\psi}(\mathbf{r}, z) = \left[\psi(r) + u(r, z)e^{ip\varphi} + v(r, z)e^{-ip\varphi}\right]e^{i(l\varphi+\beta z)} \tag{4}$$

where the perturbation functions were written explicitly in polar coordinates in order to match the description of the vortex state (2). Inserting the perturbed stationary state (4) into Eq. (1) and retaining only the first-order terms of the perturbation modes $u(r)$ and $v(r)$ we obtain an equation system which models the development of perturbations of azimuthal order p:

$$-\frac{\partial u}{\partial z} + \Delta_r u - \frac{(l+p)^2}{r^2}u + Q(\psi)u + R(\psi)v^* = 0 \tag{5a}$$

$$-\frac{\partial v}{\partial z} + \Delta_r v - \frac{(l-p)^2}{r^2}v + Q(\psi)v + R(\psi)u^* = 0 \tag{5b}$$

where $Q(\psi) = -\beta + (2n_2 - 3n_4\psi^2)\psi^2$ and $R(\psi) = (n_2 - 2n_4\psi^2)\psi^2$. The perturbation modes are characterized by an azimuthal charge p, a propagation constant δ, and the radial profiles $u(r)$, $v(r)$ of finite norm. Writing, for simplicity, $u(r, z) \equiv u(r)e^{\delta z}$ and $v(r, z) \equiv v(r)e^{\delta^* z}$ we arrive at the following linear eigenvalue problem:

$$\Delta_r u - \frac{(l+p)^2}{r^2}u + Q(\psi)u + R(\psi)v^* - \delta u = 0 \tag{6a}$$

$$\Delta_r v - \frac{(l-p)^2}{r^2}v + Q(\psi)v + R(\psi)u^* - \delta^* v = 0 \tag{6b}$$

Both the evolutionary (5) and eigenvalue (6) equations systems are the basis of the linear stability analysis. Since the radial profiles u, v and perturbation eigenvalue δ value may take on complex values throughout the numerical calculations we make no assumption concerning their realness. Numerical simulation of the propagation by Eqs. (5) offers a direct insight of physical significance of the unstable perturbation modes as they grow with the propagation distance z. The eigenvalues δ obtained from the linear eigenvalue problem (6) characterize the evolution with the propagation distance as follows [3]: whenever $\mathrm{Re}\{\delta\} > 0$ we speak of growing perturbation modes, otherwise of stable, albeit oscillatory, modes. When dealing with growing perturbation modes, the magnitude of the nonzero real part of the eigenvalue δ gives an estimation of the propagation distance by which the instability sets in while the azimuthal order p offers a qualitative description of the pattern developed by the instability during propagation [6].

In general the linear stability analysis accounts for a qualitative description of the destabilization process only during its first stage, as other types of instabilities may take over and ultimately drive the process [7].

3.2. Numerical methods for linear stability analysis

The straightforward numerical solution to the linear stability analysis is given by algorithms for eigenvalue problems applied directly to Eqs. (6) based, for instance, on finite difference [18] or spectral formulation [21]. These methods present the advantage of being applicable to a general kind of eigenvalues, including those with vanishing real part which are particularly difficult to calculate using other methods since they are oscillatory modes which do not induce growing instabilities in the stationary state. Unfortunately, they have the drawback of being unable to distinguish between physical eigenvalues and spurious ones [21]. Though there exist extra techniques [22,21] to help choosing among them they are not always applicable and a general problem may result difficult to solve. Apart from this fact a direct calculation may require a big computational effort. That is why specific methods have been developed for different systems, based on the knowledge of the kind of the perturbations that may affect the system, usually related to the symmetries. For instance, the stability of vortex states (Eq. (2)) is studied usually in polar coordinates instead of Cartesian ones, as it can be formulated by one-dimensional equations in the radial coordinate.

Some insight into the linear stability can be gained using a merely phenomenological approach where an arbitrary initial state is propagated by Eqs. (6) [4]. After a long enough propagation distance the initial data should converge to the eigenvector with the highest growth rate, and this rate is obtained comparing the amplitude of the perturbation in two consecutive positions. However, this method is not so efficient depending on the system. In such a case, due to the small growth rate, a long propagation distance and a small propagation step is necessary and the algorithm takes a long time to converge. Besides, for some systems – remarkably for the top-flat states of the cubic–quintic nonlinearity – a very dense mesh to sample the eigenstate is required and consequently the computational effort is very high [13]. As an additional drawback, this method provides only the dominant perturbation, i.e. the perturbation with greatest growth rate, masking the slower developing perturbations, and is consequently inappropriate for calculating the eigenvalues with vanishing real part (oscillatory modes [23]).

4. Relaxation algorithm

Both stationary Eq. (3) and the eigenvalue problem (6) can be reformulated in terms of a two-point boundary-value problem as follows:

$$F(\xi; \beta) = 0, \quad \text{with } \xi : [r_{min}, r_{max}] \to \mathbb{C}^n \tag{7a}$$

$$G_1(\xi, r_{min}) = 0, \qquad G_2(\xi, r_{max}) = 0 \tag{7b}$$

For the stationary equation of the vortex state we set $\xi \equiv \psi$ so that $F(\psi; \beta) = 0$ stands for Eq. (3). To operate with the eigenvalue problem we set $\xi \equiv (u, v, \delta)$ and add the differential equation $d\delta/dr = 0$ for the complex eigenvalue δ to Eqs. (6) in order to obtain $F(u, v, \delta; \beta) = 0$. With this type of parameterization we ensure that both problems can be handled automatically using the same numerical procedure. The relaxation method for the two-point boundary value problem is based on the Newton iteration method to produce successive corrections over an initial data set $\xi^{(0)}$ until a convergence criteria is met [8]:

$$\xi^{(k+1)} = \xi^{(k)} - \Delta\xi \tag{8a}$$

$$\nabla F\left(\xi^{(k)}; \beta\right) \cdot \Delta\xi = F\left(\xi^{(k)}; \beta\right) \tag{8b}$$

For an efficient numerical implementation, Eqs. (3), (8) and (6) were discretized using a second-order finite difference scheme – see Ref. [8] for details. For each value of the propagation constant β the relaxation algorithm is used to calculate the vortex eigenstate of Eq. (3) and subsequently the perturbation modes u, v and eigenvalue δ from Eqs. (6). The flowchart presented in Fig. 2 gives an overview of the adaptive procedure developed around the relaxation algorithm to follow the changes of the perturbation eigenvalue δ with the propagation constant β.

4.1. Boundary conditions

The boundary conditions (7b) derived from the asymptotic behavior of Eqs. (3) and (6) for $r_{min} \to 0$ and $r_{max} \to \infty$ read for the nonlinear vortex state ψ as:

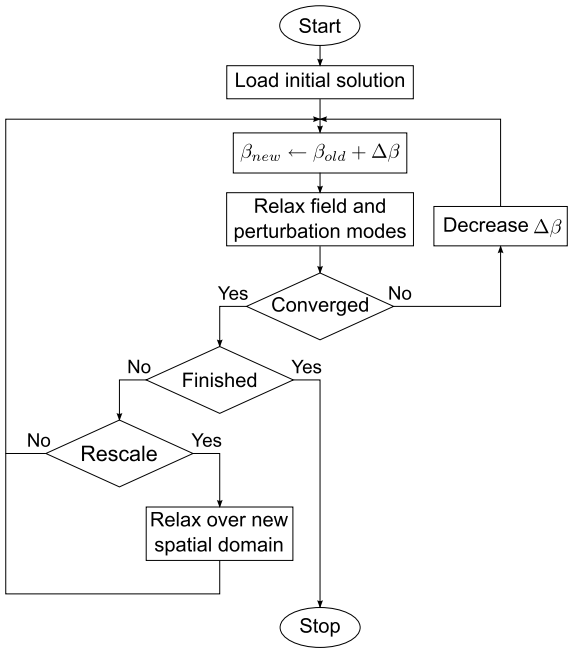

Fig. 2. Flowchart of the numerical adaptive procedure to track the perturbation eigenvalues in the linear stability analysis.

$$\psi(r \simeq r_{min}) \propto r^{|l|} \tag{9a}$$

$$\psi(r \simeq r_{max}) \propto \frac{e^{-\sqrt{\beta}r}}{r} \tag{9b}$$

and for the perturbation eigenmodes u and v as:

$$u(r \simeq r_{min}) \propto r^{|l+p|} \tag{10a}$$

$$v(r \simeq r_{min}) \propto r^{|l-p|} \tag{10b}$$

$$u(r \simeq r_{max}) \propto \frac{e^{-\sqrt{\beta - i\delta}r}}{r} = \frac{e^{(a_1+ia_2)r}}{r} \tag{10c}$$

$$v(r \simeq r_{max}) \propto \frac{e^{-\sqrt{\beta - i\delta^*}r}}{r} = \frac{e^{(b_1+ib_2)r}}{r} \tag{10d}$$

where the coefficients a_k and b_k were calculated such that $a_1, b_1 < 0$ in order to ensure finite norm perturbation modes:

$$a_{\frac{1}{2}} = \mp\frac{\sqrt{2}}{2}\sqrt{\sqrt{(\beta+\delta_I)^2+\delta_R^2} \pm (\beta+\delta_I)} \tag{11a}$$

$$b_{\frac{1}{2}} = \mp\frac{\sqrt{2}}{2}\sqrt{\sqrt{(\beta-\delta_I)^2+\delta_R^2} \pm (\beta-\delta_I)} \tag{11b}$$

with $\delta_{R(I)}$ being the real (imaginary) part of δ.

At this point a discussion regarding the boundary conditions is in order. For the field equation $F(\psi;\beta) = 0$ the two-boundary conditions (9a) and (9b) suffice to get the relaxation algorithm working. In the case of eigenvalue problem $F(u, v, \delta; \beta) = 0$ as we included an additional differential equation for the eigenvalue δ the boundary conditions (10a)–(10d) are not enough. Therefore we impose $v(r_{max}) = v_{r_{max}}$ by taking advantage of the linearity of the problem (6). This approach opens the possibility of determining complex valued eigenvalues δ of any kind, in contrary to previous conclusions that relaxation methods cannot handle complex eigenvalues [26].

4.2. Initial guess for the starting point

To start the relaxation algorithm one needs an initial guess lying sufficiently close to the numerical solution to be computed. The advantage is that one can construct such a solution for a non-critical parameters region. In the case of Eq. (3) one starts preferably by lower values of the propagation constant β where the eigenstates resemble those of cubic NLS and a simple gaussian profile works well as initial guess, or alternatively one may assume a supergaussian ansatz for the top-flat vortices close to critical value β_{cr} [11,13].

The boundary problem for the perturbation modes u, v and eigenvalue δ is more involved and to get a good starting solution we rely on the estimation of the perturbation growth rate [4] and on a pseudo-spectral solver for eigenvalue problems [21]. Also, when available, these methods were used to crosscheck the results obtained by the relaxation algorithm.

4.3. Results and discussion

We choose as starting point the solution corresponding to propagation constant $\beta = 0.1$. From this initial value the domain of β is swept toward 0 and β_{cr}. We use a number of 50 000 sampling points which distributed within an interval of few hundred units yields an error of the order of 10^{-5}.

Fig. 3 presents the dependence of the real part of the perturbation eigenvalue on the propagation constant β for vortices of different azimuthal charge l and perturbation order p, all data being computed without using any extrapolation criteria. The relaxation algorithm permits the calculation of very small perturbation eigenvalues and one can trace more accurately the decay down to zero. This decay raised some issues on deciding whether the vortex eigenstates of CQNLS equation were linearly stable or not. Eventually it was found that choosing a poor spatially discretized domain or a not small enough advancing step gave inaccurate results when trying to compute small growth rates – see Refs. [12] and [13]. From Fig. 3 one can infer that there exist small stability windows, in accordance with the conclusions drawn in Ref. [13].

In particular, the eigenstates of CQNLS equation display a qualitative change as they approach β_{cr} and their norm increases, this fact being reflected into a slower decay of the growth rate, see Fig. 3. This change takes place at very small values of growth rate and requires an increased number of points and a smaller advancing step to be traced by the growth rate method. Using the relaxation algorithm, however, no special settings were required.

In general, the vortex states of CQNLS equation display linear perturbation modes with complex eigenvalues. It was argued [26] that the relaxation algorithm would not work for complex eigenvalues. The curves presented in Fig. 3 are only a small part of a broader picture of the linear stability analysis where oscillating and growing modes may coexist. Fig. 4 displays the dependence of both real and imaginary parts of the perturbation eigenvalue δ for a vortex state $l = 2$. It was found that the relaxation algorithm can follow the changes of a complex valued δ, including the case when its real part vanishes and the growing mode turns into an oscillating one.

4.4. Efficiency and extensions

The implementation of the continuation procedure may rely on other iterative methods as well, for instance those mentioned in Ref. [9]. Taking the linear stability problem formulated in Section 3 as test problem we performed an analysis on the robustness of the Newton relaxation algorithm in comparison to an imaginary time propagation method, namely the square operator iteration method (SOM) [17].

We choose the linear perturbation mode of charge $p = 1$ of the CQ vortex with azimuthal charge $l = 50$ for $\beta = 0.1$. This particular perturbation mode possesses a small complex eigenvalue which is difficult to be determined accurately by grow rate method

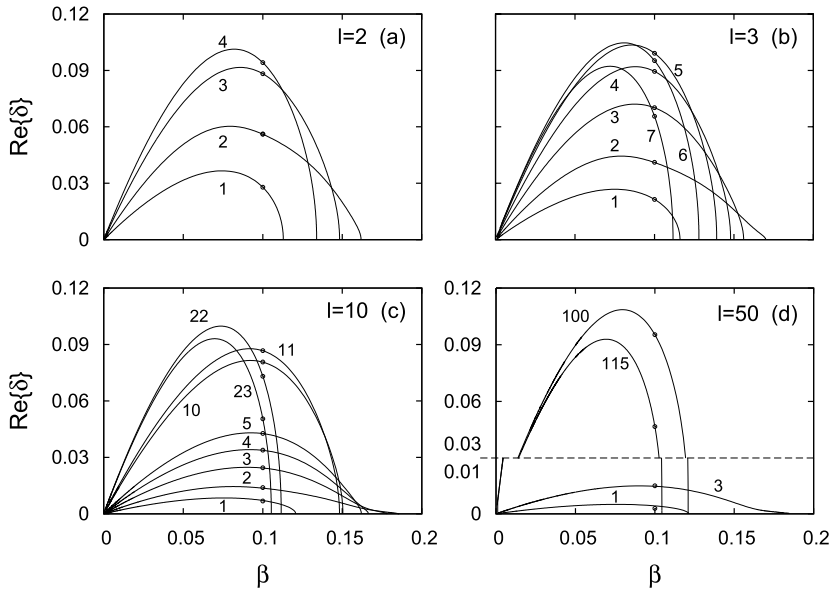

Fig. 3. (a–c) Real part of the perturbation eigenvalues for different vortices of charge l and perturbation order p (values displayed on the curves). The circles correspond to the values calculated by the growing rate method. In subfigure (d) we used a broken vertical scale in order to display the low order perturbations 1 and 3.

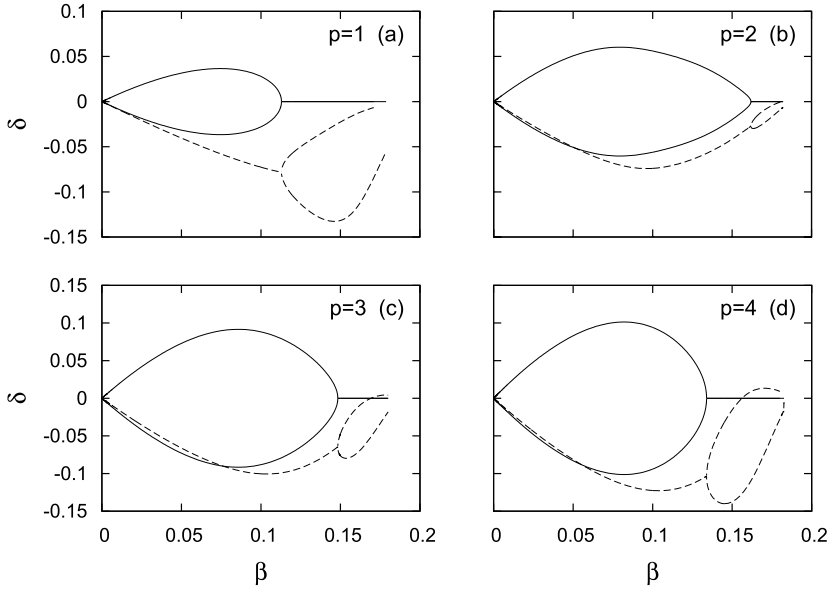

Fig. 4. Real (solid) and imaginary (dashed) part of perturbation eigenvalues for the vortex with azimuthal charge $l = 2$.

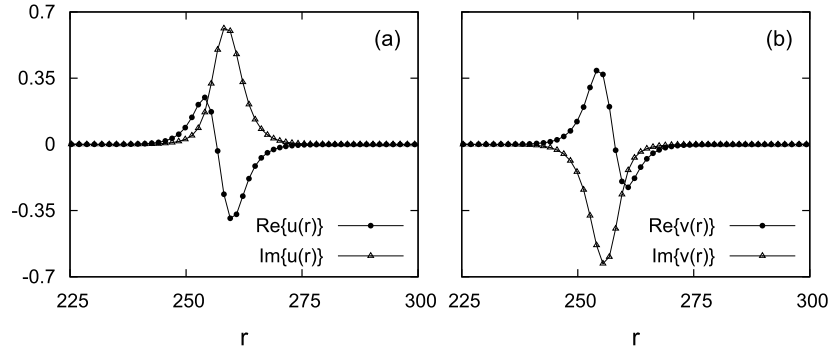

Fig. 5. Real (solid circles) and imaginary (empty triangles) part of the linear perturbation eigenmodes (a) $u(r)$ and (b) $v(r)$ of azimuthal charge $p = 1$ obtained by the direct eigenvalue method based on pseudo-spectral discretization for $\beta = 0.1$ and $l = 50$.

Table 1
Performance of Newton and SOM algorithms with respect to perturbations in the initial state. The unperturbed eigenvalue determined by the direct eigenvalue method is $\delta = (1.55333 - 3.02339i) \times 10^{-3}$. $\delta_{i(f)}$ stand for the initial (final) eigenvalue of the eigenmode.

No.	ε	$\delta_i(\times 10^{-3})$	SOM			Newton		
			Iterations	Time (s)	$\delta_f(\times 10^{-3})$	Iterations	Time (s)	$\delta_f(\times 10^{-3})$
1	10^{-5}	$1.55320 - 3.02354i$	808	30	$1.55317 - 3.02351i$	73	110	$1.42999 - 3.02439i$
2	10^{-4}	$1.55440 - 3.02534i$	4774	92	$1.55322 - 3.02465i$	73	114	$1.42999 - 3.02439i$
3	10^{-3}	$1.52559 - 2.97259i$	24509	462	$1.56594 - 2.98467i$	74	113	$1.42999 - 3.02439i$
4	10^{-2}	$1.21699 - 2.71929i$	33569	802	$1.44265 - 2.72186i$	74	115	$1.42999 - 3.02439i$
5	10^{-1}	$3.18763 - 4.80428i$	Convergence failure[a]			Convergence failure[b]		
6	–	$2.17706 - 1.46956i$	36658	841	$2.18347 - 1.38811i$	8	12	$1.42999 - 3.02439i$

[a] After approximatively 334800 iterations in 9000 second the algorithm gave as result $\delta_f \simeq (-4.0 + 0.5i) \times 10^{-3}$ which we interpreted as convergence failure.

[b] Using as initial data the perturbed pseudo-spectral eigenvectors the algorithm was not able to recover the correct eigenvalue. Nevertheless, when considering as initial data the perturbed, by same value of ε, interpolated eigenvectors the Newton algorithm converged after 9 iterations in 14 seconds to the eigenvalue $\delta_f = (1.42998 - 3.02438i) \times 10^{-3}$, line (5) in Fig. 6b.

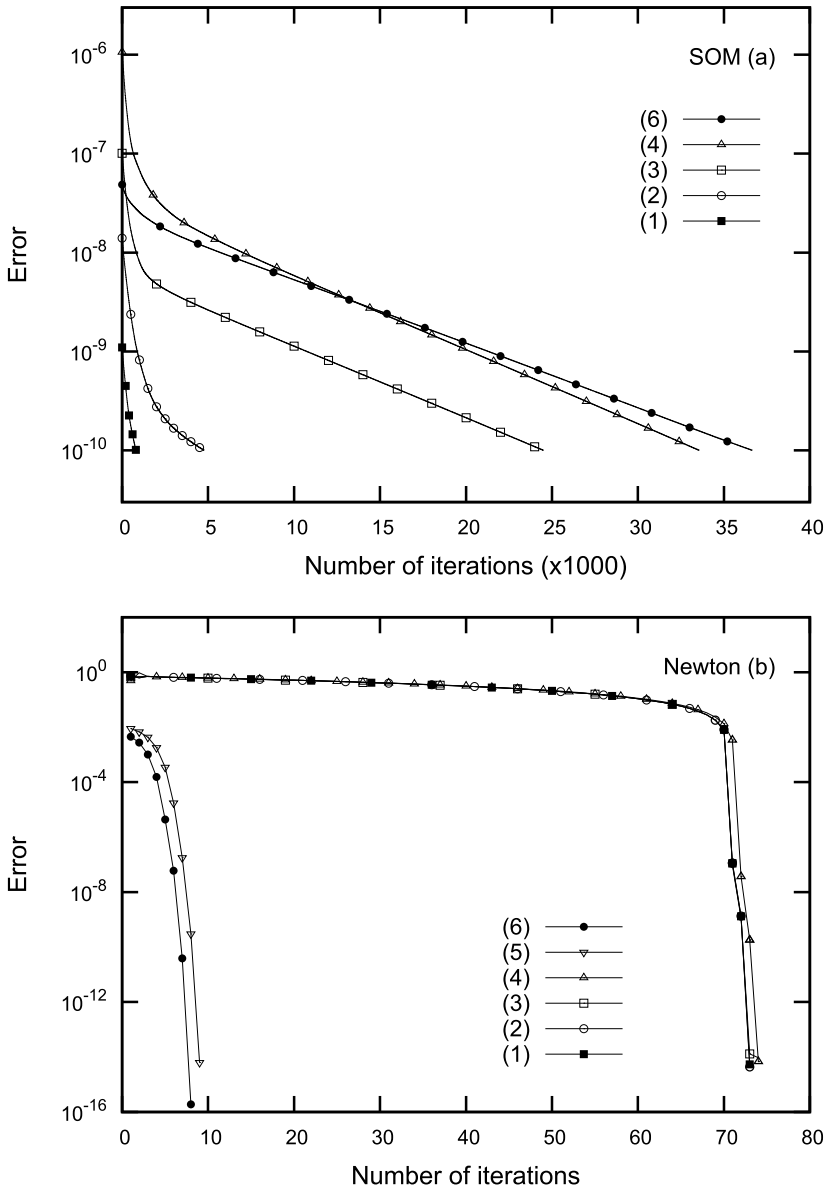

Fig. 6. Convergence of (a) SOM and (b) Newton relaxation method for several identical initial data. The line numbers correspond to the row number of Table 1. For the error definition see text.

using decent algorithm parameters. Therefore we have computed it in MATLAB directly by an eigenvalue method using a pseudo-spectral discretization. 100 collocation points generated by roots of Laguerre polynomials were displaced by a polynomial mapping function toward larger values of r in order to sample the nonlinear CQ vortex eigenstate. The spatial domain used in simulation ranges approximatively from 60 to 310. We found an eigenvalue equal to $(1.55333 - 3.02339i) \times 10^{-3}$ being validated using the technique described in Ref. [22]. Fig. 5 presents the spatial profile of the eigenmodes u and v associated to this eigenvalue.

The eigenmode computed by pseudo-spectral method is perturbed according to $\tilde{w}_j(r) = w_j(r) + \varepsilon|w_j(r)|\eta(r)$ where w_j stands for the eigenvectors u, v, and η is a random uniform distribution in the interval $[-1, 1]$. The eigenvalue corresponding to the perturbed mode was computed using the relation $\delta_i = \langle(u, v)^\dagger L(u, v)\rangle / \langle(u, v)^\dagger(u, v)\rangle$ where L represents the pseudo-spectral discretization of the linear operator defined by Eqs. (6). The perturbed mode were used as initial data for the SOM and Newton relaxation method. Table 1 resumes the information on the convergence process for several values of perturbation amplitude ε. SOM was implemented using the spatial pseudo-spectral discretization used by the direct eigenvalue method and a fourth-order Runge–Kutta method with a time-step of 10^{-2} for advancing in time. The spatial grid used in the Newton method comprises 50 000 sampling points within a radial domain of approximatively 200 units. The algorithm converged when the numerical error at step k

$$Error^{(k)} = \frac{1}{MN}\sum_{i,j=1}^{N,M}\frac{|w_j^{(k)}(r_i) - w_j^{(k-1)}(r_i)|}{\max_{r_i}|w_j^{(k-1)}(r_i)|} \tag{12}$$

drops below 10^{-10}, where N stands for the number of sampling points, $w_j(r)$ represent the radial profile involved in calculations (including the derivatives in the case of Newton method) and M for the number of radial profiles $w_j(r)$. The simulations were performed on a computer with an Intel Core 2 Duo processor working at 2.4 GHz with 4 GB RAM.

From Table 1 and Fig. 6 one remarks that the SOM converges faster than Newton relaxation for initial data lying very close, i.e. very small perturbation amplitude ε. On the other hand, Newton algorithm shows to be more robust as it converges to the same eigenvalue within the established numerical error for larger values of ε. The larger number of iterations required by the Newton algorithm is due to the fact that the spatial profile of the eigenmodes and their derivatives are constructed by linear interpolation from the initial perturbed eigenmodes. Nevertheless, when first we interpolate and then perturb the eigenmode using the same value of ε the Newton algorithm achieves very fast convergence, see note [b] of Table 1 and curve (5) in Fig. 6. As final test we used as initial data a poor approximation computed by the grow rate method using 5000 sampling points, the results are displayed on row no. 6 in Table 1 and line no. (6) in Fig. 6b.

The finite difference discretization used by the Newton relaxation algorithm restricts the accuracy of the calculations. The specific implementation of the Newton algorithm [8] allows a partial solution to this inconvenient by increasing the number of discretization points up to 10^5 as the storage needed increase linearly. However when higher precision is required from the relaxation algorithm the finite difference discretization scheme may be replaced by a (pseudo)spectral one [25]. When higher-dimensional problems are to be analyzed the same procedure as in Section 4.1 can be used in applying the boundary conditions while the eigenvalue has to fulfill $\delta(\mathbf{r}) = const$. Complications will arise as the structure of the matrix $\nabla F(\xi^{(k)}; \beta)$ changes and numerical efficient methods for linear systems like Eqs. (8) are needed [24].

5. Conclusions

We have shown that a relaxation algorithm based on Newton method allows for accurate tracing of the changes of the complex valued perturbation eigenvalues. The only requirement is an initial guess for the first perturbation eigenstate to calculate, which can be provided by a rough solution obtained by some other particular method for non-problematic values of the parameters. As an alternative to growth rate and direct eigenvalue methods, it alleviates the problem of calculating critic or problematic eigenstates since it is possible to start in a non-critic region and approach to the desired one slowly varying the parameters. Another advantage of the proposed method is the possibility of being used together with predictor–corrector, arc length continuation and bifurcation techniques in order to surpass limit and bifurcation points which may occur (for numerical implementations see for example Refs. [18,27]).

References

[1] T. Dauxois, M. Peyrard, Physics of Solitons, Cambridge University Press, UK, 2006.
[2] C. Sulem, P. Sulem, The Nonlinear Schrödinger Equation: Self-Focusing and Wave Collapse, Springer, Berlin, 2000.
[3] Yu.S. Kivshar, G.P. Agrawal, Optical Solitons: From Fibers to Photonic Crystals, Academic, San Diego, 2003.
[4] J.M. Soto-Crespo, D.R. Heatley, E.M. Wright, Phys. Rev. A 44 (1991) 636.
[5] J. Yang, D.E. Pelinovsky, Phys. Rev. E 67 (2003) 016608.
[6] M. Quiroga-Teixeiro, H. Michinel, J. Opt. Soc. Am. B 14 (1997) 2004;
B.A. Malomed, L.-C. Crasovan, D. Mihalache, Physica D 161 (2002) 187–201.
[7] A. Alexandrescu, J.R. Salgueiro, V.M. Pérez-García, H. Michinel, Phys. Rev. A 79 (2009) 063843.
[8] W.H. Press, et al., Numerical Recipes in C, Cambridge University Press, 1992.
[9] J. Yang, J. Comput. Phys. 227 (2008) 6862;
J. Yang, Nonlinear Waves in Integrable and Nonintegrable Systems, SIAM, Philadelphia, 2010.
[10] Z. Jovanovski, J. Mod. Opt. 48 (2001) 865;
H. Michinel, J. Campo-Táboas, R. García-Fernández, J.R. Salgueiro, M.L. Quiroga-Teixeiro, Phys. Rev. E 65 (2002) 066604.
[11] K. Dimitrevski, E. Reimhult, E. Svensson, A. Öhgren, D. Anderson, A. Berntson, M. Lisak, M.L. Quiroga-Teixeiro, Phys. Lett. A 248 (1998) 369.
[12] I. Towers, A.V. Buryak, R.A. Sammut, B.A. Malomed, L.C. Crasovan, D. Mihalache, Phys. Lett. A 288 (2001) 292.
[13] H. Michinel, J.R. Salgueiro, M.J. Paz-Alonso, Phys. Rev. E 70 (2004) 66605.
[14] V.I. Berezhiani, V. Skarka, N.B. Aleksić, Phys. Rev. E 64 (2001) 057601.
[15] J.J. García-Ripoll, V.M. Pérez-García, SIAM J. Sci. Comput. 23 (2001) 1315.
[16] M.J. Ablowitz, Z.H. Musslimani, Opt. Lett. 30 (2005) 2140.
[17] J. Yang, J. Comp. Phys. 228 (2009) 7007.
[18] H.B. Keller, Numerical Methods for Two-Point Boundary-Value Problems, Dover, New York, 1992.
[19] A. Alexandrescu, Ph.D. thesis, University of Castilla-La Mancha, 2009.
[20] W.J. Firth, D.V. Skryabin, Phys. Rev. Lett. 79 (1997) 2450–2453.
[21] J.P. Boyd, Chebyshev and Fourier Spectral Methods, second edn., Dover, New York, 2001.
[22] J.P. Boyd, J. Comp. Phys. 126 (1996) 11–20; Corrigendum 136 (1997) 227–228.
[23] L. Dong, F. Ye, J. Wang, T. Cai, Y.-P. Li, Physica D 194 (2004) 219–226.
[24] J.R. Salgueiro, D. Olivieri, H. Michinel, Opt. Quant. Electron. 39 (2007) 239.
[25] H.I. Tarman, H. Berberoğlu, J. Lightw. Technol. 13 (2009) 2289.
[26] I. Towers, A.V. Buryak, R.A. Sammut, B.A. Malomed, Phys. Rev. E 63 (2001) 055601(R).
[27] R. Glowinski, H.B. Keller, L. Reinhart, SIAM J. Sci. Stat. Comput. 6 (1985) 793–832;
C.T. Kelley, unpublished notes, http://www4.ncsu.edu/~ctk/MA784/continue.pdf.